UCRL-JC-118286
PREPRINT

SMART ACTIVE MULTIWAVE SENSING WITH ZERO BACKGROUND AMPLITUDE MODULATED PROBES

Anthony J. Ruggiero, Richard A. Young, and Larry Jelsma

Lawrence Livermore National Laboratory

This paper was prepared for
the Proceedings of the 1994 CALIOPE ITR Conference
held April 26-28, 1994, in Livermore, California

July 1994

SMART ACTIVE MULTIWAVE SENSING WITH ZERO BACKGROUND AMPLITUDE MODULATED PROBES

Anthony J. Ruggiero, Richard A. Young, and Larry Jelsma
Lawrence Livermore National Laboratory, Livermore, California 94551

Abstract. Recently, a new approach to multi-wavelength remote sensing has been proposed based on the generation and detection of spectral "pickets" synthesized from the frequency filtered bandwidth of a modelocked laser.[1] Using linear array liquid crystal spatial light modulator (SLM) technology for spectral filtering permits real time grey scale control of individual picket amplitudes and phases, making it possible to independently modulate picket characteristics in the kHz to MHz regime. Due to the versatility of this approach, a whole suite of spectroscopies based on detection techniques that are similar to conventional sideband spectroscopies can be implemented. These techniques not only inherit the S/N advantages of their conventional counterparts, they can also be easily extended to simultaneous multi-wavelength operation using frequency multiplex techniques and configured for real time adaptive data acquisition. We report the laboratory demonstration and theoretical development of a new class of zero background AM modulated spectroscopic probes for differential absorption measurements. Preliminary detection sensitivities on the order of 10^{-6} can be inferred from our measurements. Application of this technique to realistic remote sensing scenarios, advantages over other modulation and direct detection approaches, as well as the present limitations and theoretical limits to detection sensitivity will be discussed.

Introduction

The minimum amount of spectral information required to unambiguously identify a trace gas species in a complex effluent is strongly dependent on the data collection scenario. Sensors that can respond in real time to changes in the prevailing physical and chemical conditions of the target environment become increasingly important in situations where data acquisition time is limited, signal to noise levels are low, and countermeasures may be operative. Smart active sensors are technologies that permit this type of adaptive information retrieval. On-line spectroscopic analysis based on smart multispectral sensors, in principle allow strategies to be used for both enhancing detectability of weak spectral signatures in the presence of target specific noise as well as detailed effluent interrogation based on preprogrammed proliferation scenarios.

We are presently pursuing a two stage approach for development and implementation of a smart active multispectral sensor for remote differential optical absorption measurements. The first stage involves the development and evaluation of techniques for efficiently generating and detecting well defined, user selectable multi-wavelength optical fields. Subsequent frequency conversion and high power amplification of these probe fields to match the atmospheric windows and estimated mission range/power requirements constitutes the second stage of the work. This report will focus on recent progress on the first stage of this effort.

Using an extension of technology originally developed for optical pulse shaping applications[2], we have configured a high resolution "coherent multiwave optical seeder" for generating spectrally tailored optical fields in real time. A schematic of the device is shown in Figure 1. The seeder works by taking the fiber coupled output from a modelocked laser and spectrally dispersing it using volume phase holographic gratings. Individual frequency components of the dispersed spectrum are then filtered or modulated with regard to optical phase, amplitude or both using high speed voltage programmable linear array spatial light modulators (SLM's). The dispersed light is then spatially recombined into a single beam with a second grating oriented for negative dispersion and launched into the output fiber.

Grey scale control of the individual SLM pixels is presently possible with millisecond to microsecond response times. The faster microsecond response devices are non-commercial experimental SLM's being tested and developed at LLNL for this application. Multiple wavelengths or spectral “pickets” can be selected for simultaneous output over a spectral range determined by the available modelocked bandwidth, while the total number of selectable wavelength channels is dependent on the SLM array size (nominally 128-256 pixels, extendable to 1024 pixels). The linewidth of the individual spectral pickets is determined by the grating dispersion, optical geometry and SLM pixel size. For reasonably compact optical geometry's, standard gratings and pixel sizes of 4-100 μm, spectral resolution on the order of 1-30 GHz/pixel is easily obtainable. Higher spectral resolution is possible in principle, by placing individual laser longitudinal modes in each pixel. Operating in this mode, the spectral resolution of the seeder would be determined by the linewidth of the individual longitudinal modes of the source. Interestingly, for an ideally modelocked laser, the linewidth of each of the locked modes is equivalent to a single mode laser operating at the same average power[3] (sub-MHz in this case). Consequently, the seeder in this configuration could be thought of as a phase locked multi-wavelength array of single mode lasers. Larger synthetic picket linewidths if desired can be generated by binning multiple pixels.

Producing spectrally encoded optical fields in this manner lends itself to numerous possibilities for making adaptive spectroscopic measurements. One option is simply the straight forward extension of conventional DIAL to measurements of multiple on and off resonant wavelength pairs by direct multichannel detection of the spectrally dispersed signal returns. In certain situations, autodyne techniques based on measurements of heterodyne beat frequencies between spectral pickets could also be used. This latter technique has been demonstrated in our laboratory.[4] Taking advantage of our ability to independently AM or FM modulate individual SLM pixels in kHz to MHz regime permits both autodyne detection at lower frequencies than the pixel spacing, along with a whole suite of spectroscopies based on operation of the SLM pixels concurrently as spectral filters and RF frequency tunable n-channel optical phase or amplitude modulators. Coherent detection approaches alone or in combination with selected modulation formats form a third, yet unexplored detection option. We are particularly interested in the modulation techniques, since in principle they can offer several practical advantages over direct detection of dispersed light. Characterized by high throughput, high spectral resolution, and narrow detection bandwidths, these techniques potentially offer quantum limited detection sensitivities. Easily configured for simultaneous multi-wavelength data acquisition via narrow band frequency multiplex detection with a single compact detector, modulation approaches also eliminate the need for a high resolution spectrometer or narrow band optical filters for background noise rejection. A major consideration, however, in evaluating the benefits and feasibility of their use in remote sensing applications involves the effects of target induced speckle and atmospheric turbulence on the return signals. Speckle noise can result from pathlength fluctuations on both the optical wavelength and modulation wavelength scales. Consequently, long range chemical remote sensing employing topographic backscatter will require relatively low modulation frequencies (MHz-kHz) to minimize the latter contribution. A more quantitative estimate of the magnitude of these effects will be discussed later. It can be anticipated that in situations where the speckle noise contribution to the measurement signal to noise ratio is the same as for direct detection, using modulation techniques will offer a substantial practical advantage. Both measurement approaches however will require signal averaging to achieve the required detection sensitivities in the presence of target induced speckle.

This report deals with the initial laboratory demonstration and development of a new class of multi-wavelength zero background amplitude modulated spectroscopic probes. These probes represent one of several possible detection techniques we are evaluating in an iterative fashion for a field deployable smart active multiwave sensor. We expect to modify and refine our approach as our knowledge of mission specific problems evolve and our experience in the field increases.

Measurement Theory

The AM modulated spectrographic probes described here are similar in concept to those based on two tone frequency modulation spectroscopy.[5] Both methods provide a signal that shifts away from a null when one wavelength (or sideband) is absorbed by a spectral feature of interest. In both cases, the signal is detected at a lower frequency than the difference between on and off resonant wavelengths. In the AM case, the signals arise from two equal intensity modulated carriers whose sidebands are shifted 180 degrees with respect to each other as indicated in Figure 2. This is accomplished by alternately switching on and off selected SLM pixels corresponding to the desired optical wavelengths at the same RF modulation frequency. Pixel intensities are initially balanced using the grey scale amplitude control. A schematic of the balanced modulation scheme is shown in Figure 3. The two wavelength AM probe field generated in this fashion is then represented by

$$\begin{aligned} E(t) = E_c(1 - M\cos(\omega_m t + \Gamma))\cos(\omega_{c1} t + \theta_1) + \\ E_c(1 + M\cos(\omega_m t + \Gamma))\cos(\omega_{c2} t + \theta_2) \end{aligned} \tag{1}$$

where E_1=E_2=E_c is the balanced source field amplitude at optical frequencies ω_1 and ω_2, with optical phases θ_1 and θ_2, modulation index M, and RF modulation frequency ω_m.

After propagation and scattering off the target, the spectroscopically modified probe field is given by

$$\begin{aligned} E(t) = E_c T_1 S_1(t)\left(1 - M\cos\left(\omega_m t + \Gamma(t)\right)\right) \cos\left(\omega_{c1} t + \theta_1\right) + \\ E_c T_2 S_2(t)\left(1 + M\cos\left(\omega_m t + \Gamma(t)\right)\right) \cos\left(\omega_{c2} t + \theta_2\right) \end{aligned} \tag{2}$$

with transmission coefficients T_1 and T_2 defined in terms of the amplitude attenuation δ_n, at optical triplet n by $T_n = T_0 \exp(-\delta_n)$. The pre-exponential factor $T_0 = \exp(\delta_0)$, accounts for any possible broadband background attenuation, while $S_1(t)$ and $S_2(t)$ represent speckle loss coefficients that describe amplitude fluctuations due to changes in the wavelength dependent speckle patterns over the detection aperture. $\theta_1(t)$ and $\theta_2(t)$ are gaussian random variables that describe the propagation and dispersive phase shifts occurring over range R and for dispersion ϕ near absorption features, and are defined by $\theta_n = [(2\omega_c R)/c] + \phi$]. $\Gamma(t)$ is the modulation phase shift, due to propagation path differences is given by $\Gamma = (2\omega_m R)/c$. Optical frequency separations on the order of 5-10 GHz between modulation triplets and modulation frequencies in the kHz to MHz frequency range are assumed. It is also assumed that the losses and relative phase shifts of the modulation terms with respect to the carrier are the same for optical frequency components of the modulation triplets, *i.e.* the phase of the carrier frequency and sideband terms for the resonant triplet are shifted equal amounts by the absorption feature being probed and the speckle patterns and propagation effects for frequency components within the triplets are highly correlated. The validity of this assumption will be discussed in more detail later. The intensity incident on the photodetector is then

$$\mathrm{I}(\mathrm{t}) = \frac{c}{8\pi}\left|\mathrm{E}(\mathrm{t})\right|^2 \tag{3}$$

and the component of the irradiance at the beat frequency, ω_m, is

$$\mathrm{I_{RF}}(\mathrm{t}) = \frac{c}{8\pi}\ \mathrm{M}\ \mathrm{E_c^2}\left[-\left(\mathrm{T_1S_1}(\mathrm{t})\right)^2 + \left(\mathrm{T_2S_2}(\mathrm{t})\right)^2\right]\cos\left(\omega_{\mathrm{m}}\mathrm{t} + \Gamma(\mathrm{t})\right) \tag{4}$$

The signal current detected at ω_m obtained by filtering the DC and high frequency components is then proportional to

$$i_{\mathrm{s}}(\mathrm{t}) = \left(\frac{e\eta}{h\nu}\right)\mathrm{A_d I_{RF}}(\mathrm{t}) \tag{5}$$

in terms of detector area A_d, electric charge, *e,* detector quantum efficiency η, and quantum energy $h\nu$. For weak absorptions ($\delta << 1$) and no speckle noise,

$$i_{\mathrm{s}}(\mathrm{t}) = \left(\frac{e\eta}{h\nu}\right)\mathrm{P_0}\ \mathrm{M}\ \exp\left(-2\delta_0\right)2\left(\delta_2 - \delta_1\right)\cos\left(\omega_{\mathrm{m}}\mathrm{t} + \Gamma(\mathrm{t})\right) \tag{6}$$

where P_o is the average detected power of the two optical triplets. By balancing the modulation index and optical power at both wavelengths, zero background detection is possible. It is useful to note that the signal is linear in modulation index as opposed to the quadratic dependence of the conventional two tone FM measurement. An AM modulation index of one will result in a signal two orders of magnitude greater than the traditional FM case which is limited by operational constraints to indexes of approximately 0.1. Loss of the null condition due to residual AM resulting from a picket imbalance at the source can be removed by simultaneous subtraction of a reference field with a balanced detector. The presence of speckle noise induced amplitude fluctuations at the on/off resonant wavelengths, will also destroy the instantaneous detection null, but conventional speckle averaging techniques should be effective in its recovery as long as the measurements are made in a fashion that preserve the sign of the fluctuations. This is easily achieved using a RF Fourier signal analyzer.

The discussion so far has focused on two wavelength single mode AM probes, it is useful to extend the measurement theory to include expressions for AM signals recovered with multi-mode spectral pickets, as was the case for the experimental results that have been obtained thus far, and for multiple AM picket pairs, the extension to true multiwave operation. For spectral pickets composed of N+1 longitudinal modes spaced by ω_r, that are symmetric about the laser picket frequency ω_{ck}, the optical field is described by

$$E_{ck} = \mathrm{Re}\left(\sum_{n=-N/2}^{N/2} E_n \exp\left\{ i\left[\left(\omega_{ck} + n\omega_r \right) t + \phi_n \right] \right\} \right) \tag{7}$$

where E_{nk} is the real amplitude of the n^{th} laser mode in the k^{th} spectral picket and ϕ_n is its phase. Assuming the average intensity of both pickets are balanced and the modes and their modulation sidebands within a picket experience the same relative phase shifts, substituting Equation 7 into Equation 2 and then calculating the component of the irradiance at the beat frequency, ω_m, yields

$$I_{RF}(t) = \frac{c}{8\pi} M \left[-\sum_n E_{n1}^2 \left(T_{n1} S_{n1}(t) \right)^2 + \sum_n E_{n2}^2 \left(T_{n2} S_{n2}(t) \right)^2 \right] \cos\left(\omega_m t + \Gamma(t) \right) \tag{8}$$

Since only neighboring sidebands of the same mode have a frequency difference of ω_m and contribute to the homodyne detected signal, the multimode picket AM signal is simply the sum of the individual AM signals from each mode, weighted by the power in that mode. The RF component of the irradiance from zero background AM probes composed of multiple pairs of balanced pickets modulated at different RF modulation frequencies can be expressed as

$$I_{RF}(t) = \frac{c}{8\pi} M \sum_k E_k^2 \left[-\left(T_k S_k(t) \right)^2 + \left(T_{k'} S_{k'}(t) \right)^2 \right] \cos\left(\omega_{mk} t + \Gamma(t) \right) \tag{9}$$

where k and k' are pairs of balanced optical pickets with modulation frequency ω_{mk}. A key feature of this result is that it suggests the possibility of simultaneous multi-spectral data acquisition using narrow band RF frequency multiplex detection techniques. In this case, the optical difference frequencies are mapped into corresponding RF frequencies for detection. An illustration of this mode of operation as applied to simultaneous differential absorption measurements of two spectroscopic features is shown in Figure 4. Alternately, a scanning mode of operation could be implemented by sequentially changing the SLM pixels corresponding to the optical wavelengths of interest and using a single RF modulation frequency for detection.

Experimental Results

The experimental geometry for laboratory feasibility studies and S/N measurements of differential absorption using the proposed zero background AM probes is shown in Figure 5. A diode pumped 100 MHz modelocked mini-Nd:YAG laser operating at 1064 nm was used as the source for this work. For demonstration purposes, spectrally formatted light from the fiber coupled output of the coherent multiwave seeder was propagated to a 500 MHz bandwidth Burleigh etalon used in reflection mode to mimic a 3% absorption of one of the spectral pickets. Reflected light from the etalon was then detected with a New Focus 1811 photodetector. The AM component of the signal was measured with an HP 89410A vector signal analyzer. Spectral and temporal diagnostics of the tailored optical fields were obtained with a 6000 GHz free spectral range SR250 Newport Corp. supercavity optical spectrum analyzer and a New Focus model 1014 photodetector / CSA803 digital sampling oscilloscope combination respectively. A separate New Focus 1811 was used for experiments involving removal of residual AM due to source picket imbalances by balanced detection. Placement of an interferometer arrangement prior to the sample etalon and diagnostics allowed the effects on the AM signals of fading due to interference effects (pathlength variations) on the order of the picket separation to be examined. Examples of a pair of modelocked 10 GHz linewidth multimode spectral pickets generated by frequency domain filtering with the sample etalon on and off resonance are shown in Figures 6a and 6b. The pickets are separated by 35 GHz. Zero background operation of the AM differential absorption technique is demonstrated in Figure 7a and 7b for detection of the 3% etalon absorption. Signal data plotted on a log scale for this measurement is shown in Figure 8. The data corresponds to 10 micro-watts of detected laser power, a 7 second integration time with a 3Hz detection bandwidth and a 20 MHz modulation frequency. Signal to noise for this measurement as determined from the signal peak and RMS background noise calculated directly by the HP89410A vector signal analyzer is 4×10^3. Extrapolating to a S/N = 1 and a standard detection bandwidth of 1 Hz, the estimated detection limit of our current experimental arrangement is $[\alpha/SNR_{meas}]\ (BW)^{-1/2} = 1.5 \times 10^{-6}$. Measurements of the theoretical predicted signal linearity as a function of detected optical power and AM modulation index are shown in Figures 9 and 10. To verify the insensitivity of the AM signal to propagation pathlength variations on the order of the 35 GHz picket separation, we used the input interferometer referred to earlier, to generate two zero background AM probe fields with an optical path difference that resulted in GHz photocurrent beat signals 180 degrees out of phase. This simulated situation, would correspond for example, to photocurrent beats resulting from differently phased speckle lobes within the detection aperture. It is equivalent to maintaining the relative phases of the frequency components (longitudinal mode triplets) within the picket but shifting the relative phase of the two pickets with respect to each other. As can be seen in Figure 11, although the temporal beats in the photocurrent at the GHz frequency spacing of the spectral pickets has been virtually eliminated by the two interfering probe beams, the RF AM signal is unchanged. This is consistent with Expression 2 for the AM signal which indicates that the received AM signals will be independent of the carrier phase fluctuations as long as the relative phase of the modulation sidebands is maintained. Signals will depend on variations in the modulation phase shift $\Delta\Gamma=2\Delta R\omega_m/c$ where ω_m is the modulation frequency. For kHz-MHz modulation frequencies, the modulation phase shift caused by a change in range *i.e.*, multipath or phase “clutter” effects will be insignificant since they will require pathlength variations on the order of 300 meters or greater.

Discussion

To summarize, the zero background AM technique we have developed and demonstrated in the laboratory has the detection advantages typically associated with conventional two tone FM spectroscopy. It is a zero background technique in speckle free conditions. In situations where target induced speckle noise dominates, however, speckle averaging will be necessary to recover the null. The use of modulation frequencies in the kHz to MHz range permit the use of readily available low bandwidth detectors with reduced electronic noise and large active areas. Signal fluctuations due to pathlength induced phase clutter at these modulation frequencies will be insignificant, since in this modulation frequency regime, pathlength variations on the order of 300 meters would be necessary to have an effect. The major advantage of the AM detection system is that the return signal is linear in modulation index as compared to the quadratic dependence found for traditional two tone FM techniques. As mentioned earlier, the AM system will have at least two orders of magnitude greater signal level when compared to a traditional two tone FM system. The main limitation of the AM system as configured is that the modulation frequency amplitudes must be manually adjusted to achieve a balance where as the FM sidebands are in principle self adjusting. This does not appear to be a major concern since we are able to obtain reasonable balance even in the substantially less than optimal conditions that were used for these initial experiments. We are presently developing an electronic SLM driver that will enable us to fine tune the amplitude balance to compensate for both electronic as well as SLM pixel inhomogeneities that effect the modulation index. Perhaps, the greatest advantage of this technique is that it is easily extendable to multispectral data acquisition since different kHz-MHz amplitude or phase modulation frequencies can trivially be applied to different on/off resonant pixel pairs and the resulting difference spectra detected with a narrowband RF spectrum analyzer.

Our ability to maintain an averaged null background condition in an actual remote sensing scenario can be explored by examining the cross-correlation function of speckle patterns differing by the MHz to kHz separations proposed here. A very conservative estimate of this function can be obtained using the normalized form of the spectral correlation function for a circular aperture and a scattering surface characterized by a gaussian height distribution of scatterers. The extent of decorrelation between optical frequency components of a given AM probe triplet can be obtained from the following expression [6]

$$1-e^{-2\pi^2\delta\omega^2\sigma_z{}^2} \tag{10}$$

where σ_Z is the rms surface height including contributions due to tilt of the scattering surface, and $\delta\omega$, is the frequency difference in wavenumbers ($1/\lambda$). For a one meter spot size, the decorrelation would be on the order of 2×10^{-4}, for a 1 MHz spectral separation, 5×10^{-5} for a 500 kHz separation and 2×10^{-6}, for a 100 kHz spectral separation between optical frequency components. These values place a noise floor on the null obtained with the zero background measurement. S/N would still be improved by speckle averaging. Effects due to atmospheric turbulence decorrelate with wavelength difference much more slowly than target induced speckle and are expected to be insignificant for the MHz spectral separations and scenarios discussed here.[7] It is interesting to note however that the decorrelation is linear in wavelength difference and in principle, turbulence induced noise could be removed by comparing intensities at more than two wavelengths.[8] Since the RF modulation frequencies proposed here are very small compared to the Doppler-broadened absorption lines of interest, all frequencies of a sideband group will suffer approximately the same absorption and dispersion at the target.

Future Directions

We are currently in the process of improving the detection sensitivity of the zero background AM probes that have been described. Improvements of one to two orders of magnitude in laboratory detection sensitivity as well as quantum limited performance are anticipated. Further system optimization and investigations of data extraction from signals corrupted with injected RF phase and amplitude noise, *i.e.* laboratory generated speckle noise are also planned to prepare for actual field experiments. The hardware is almost complete for demonstrating zero background AM operation at eight simultaneous optical wavelengths, with variable spectral separations, corresponding to four RF detection frequencies. We are also presently investigating techniques for simultaneously monitoring the averaged received power per AM probe pair along with their differential absorptions.

Whereas the experiments described here use quasi continuous repetitive measurements, ultimately a burst mode operation and detection with gated spectral analysis may be required for high power operation, this is another area under study. As mentioned in the introduction, the second stage of this work will be concerned with frequency conversion and amplification of multiwave RF modulated laser fields. Concurrent with these efforts, higher spectral resolution and more compact multiwave seeder architecture's are being explored.

Acknowledgments

We would like to thank Jim Morris for very enlightening discussions on the topics of target induced speckle and beam propagation effects. We would also like to acknowledge Mike Staggs and Jerry Benterou for general laboratory support on the CALIOPE projects. Research described in this article was performed under the auspices of the U.S. Department of Energy by Lawrence Livermore National Laboratories under contract No. W-7405-ENG-48.

References

1. Anthony J. Ruggiero, "*Programmable Spectral Wavepacket Differential Absorption and Imaging*", Disclosure and Record of Invention, IL-9270, Lawrence Livermore National Laboratory, May 1993.

2. A.M. Weiner, J.P. Heritage, and E.M. Kirshner, "High Resolution Femtosecond Pulse Shaping", J. Opt. Soc. Am. B., 5, (8), p.1563-1572, 1988. and references there in.

3. P.T. Ho, "Phase and Amplitude Fluctuations in a Modelocked Laser", IEEE J. Quantum Electronics, QE-21, 11, p.1806-1813, 1985.

4. Anthony J. Ruggiero, "*Smart Active Sensors for Multispectral Differential Absorption Using Modelocked Pulses*", JASON CALIOPE Review, La Jolla, CA, June 15, 1993.

5. G. R. Janik C. B. Carlisle, and T. F. Gallagher, J. Opt. Soc. Am. B, Vol. 3, No. 8, pp. 1070-1074, 1986.

6. G. Parry, "*Speckle Patterns in Partially Coherent Light*", <u>Laser Speckle and Related Phenomena,</u> Ed. J.C. Dainty, Springer Verlag, New York,1984.

7.Clifford, S.F., "*Classical Theory of Wave Propagation in a Turbulent Medium*," in <u>Laser Beam Propagation in the Atmosphere</u>, ed. J.W. Strohbehn, New York: Springer p.9, 1978.

8. "*LIDAR*", JSR-93-310, JASON, The MITRE Corporation, pp. 44-52, November, 1993.

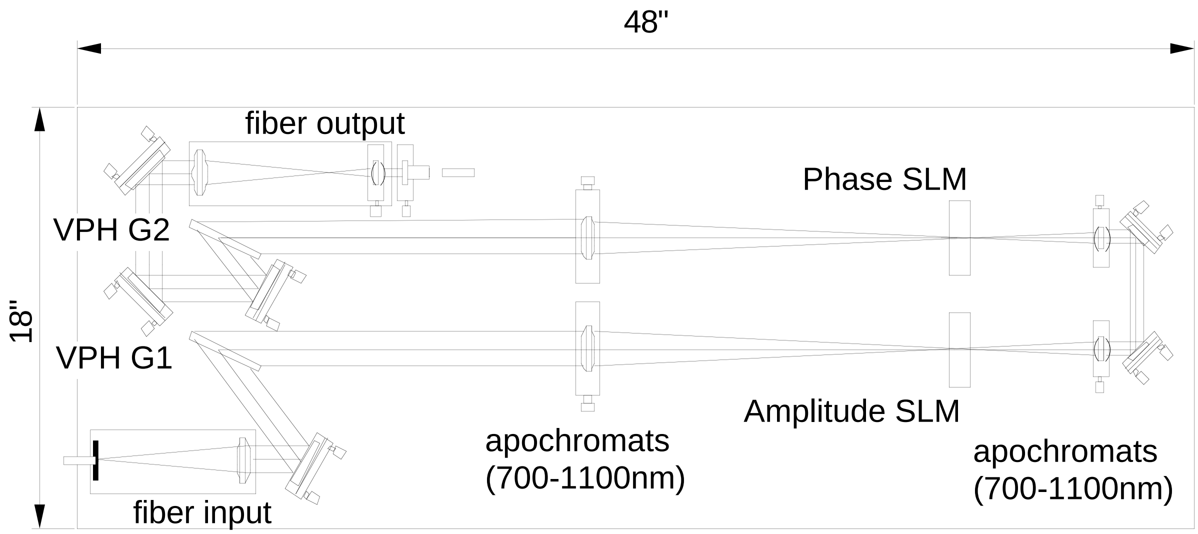

Figure 1. Schematic diagram for the coherent multi-wave seeder.

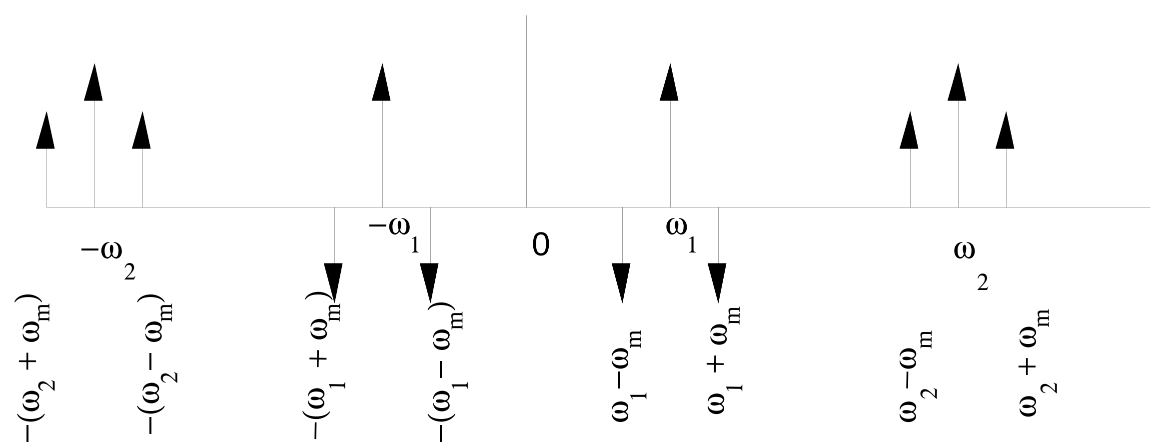

Figure 2. Spectral representation of a two wavelength AM probe field.

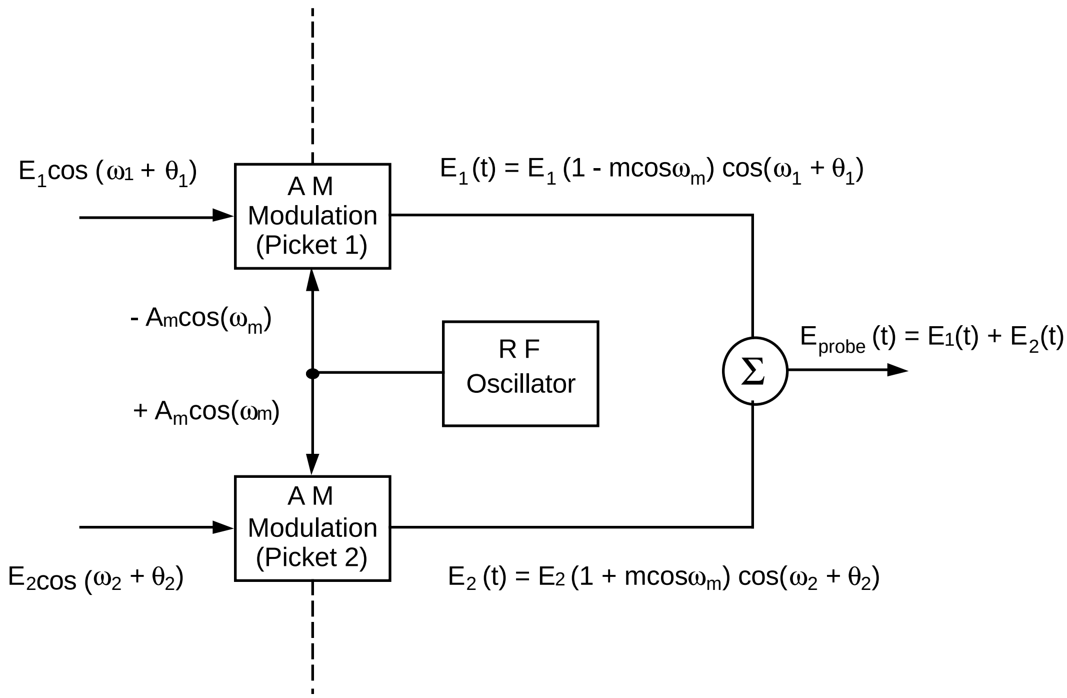

Figure 3. Zero background AM generation schematic.

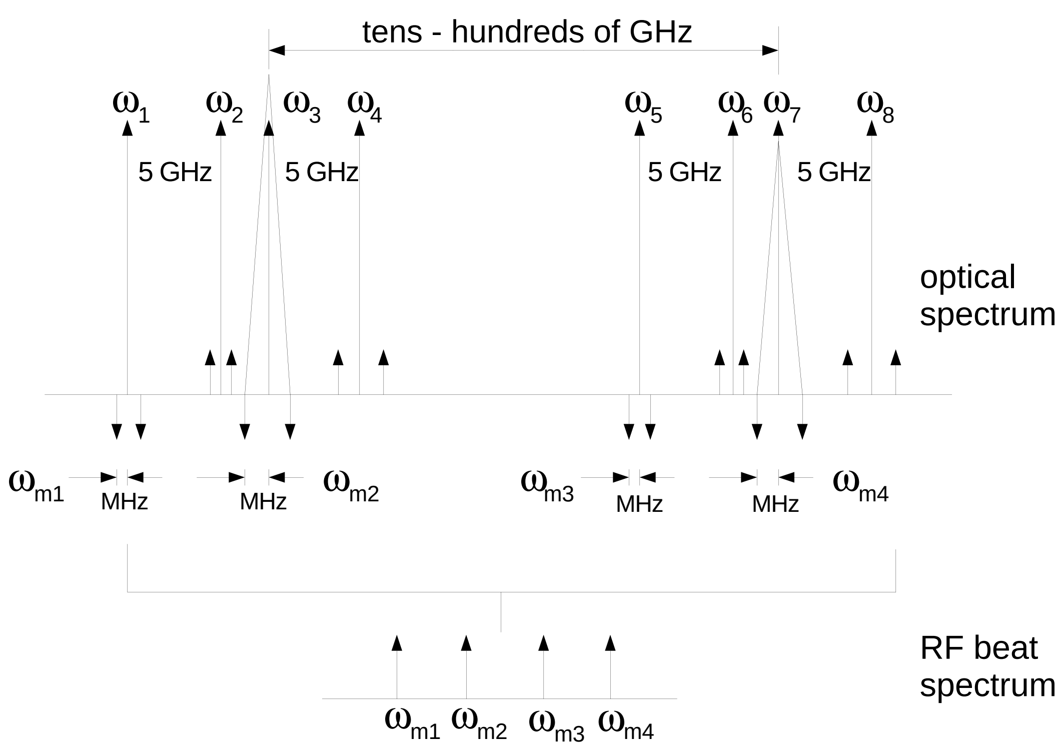

Figure 4. RF frequency multiplex detection of the AM signals permits simultaneous multispectral data acquisition.

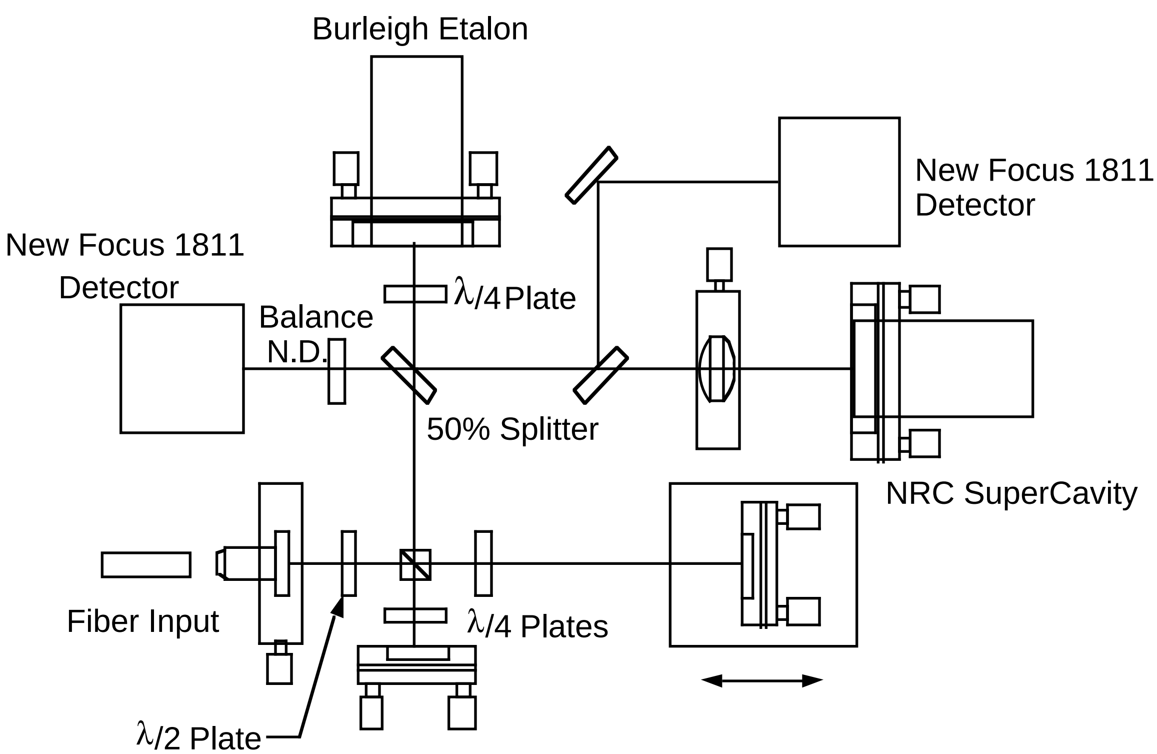

Figure 5. Experimental geometry for S/N and GHz fading measurements. Details are given in the text.

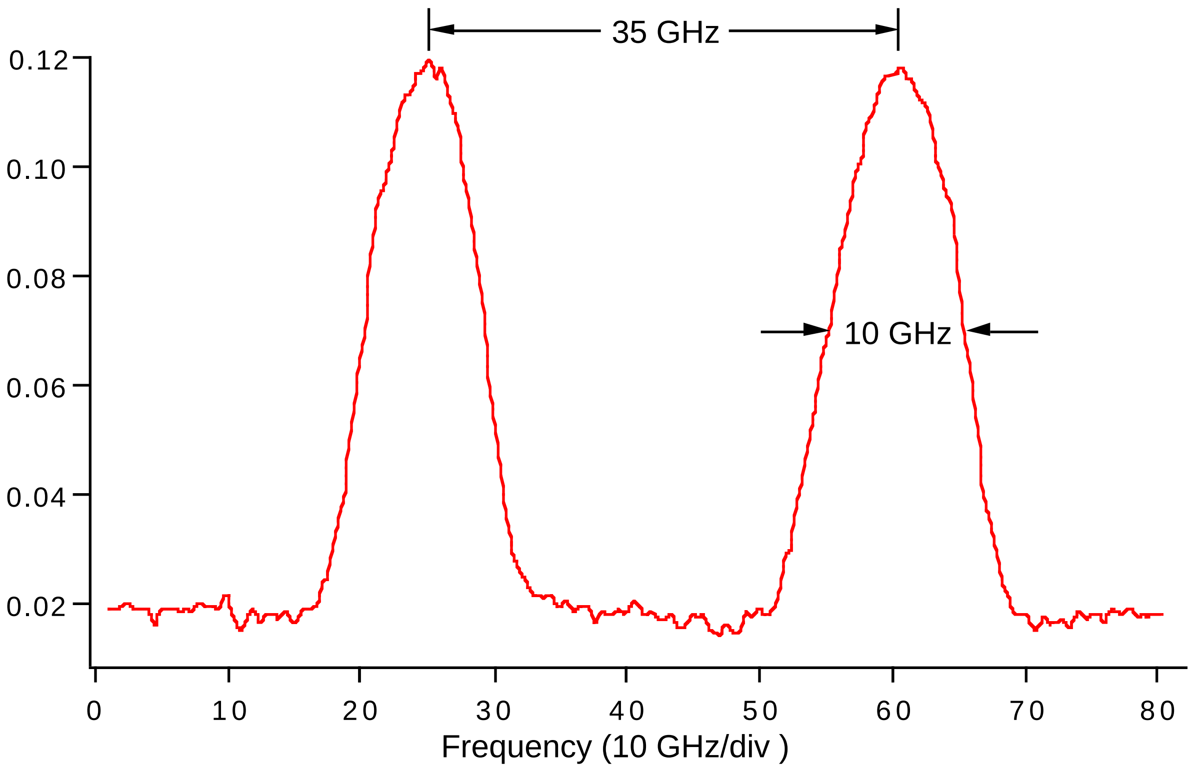

Figure 6a. Multimode pickets crafted from a modelocked Nd:YAG laser by frequency domain filtering at 1064 nm.

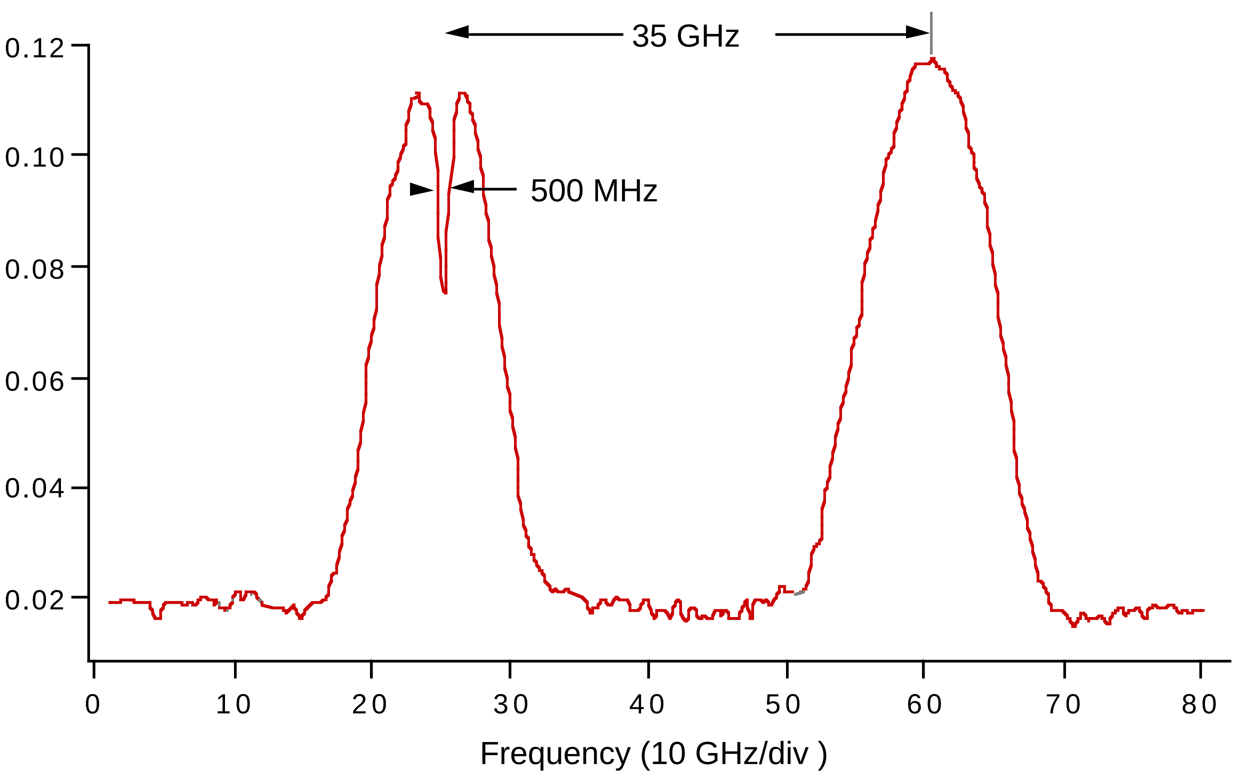

Figure 6b. Nd:YAG picket with 3% absorption from sample etalon on resonance.

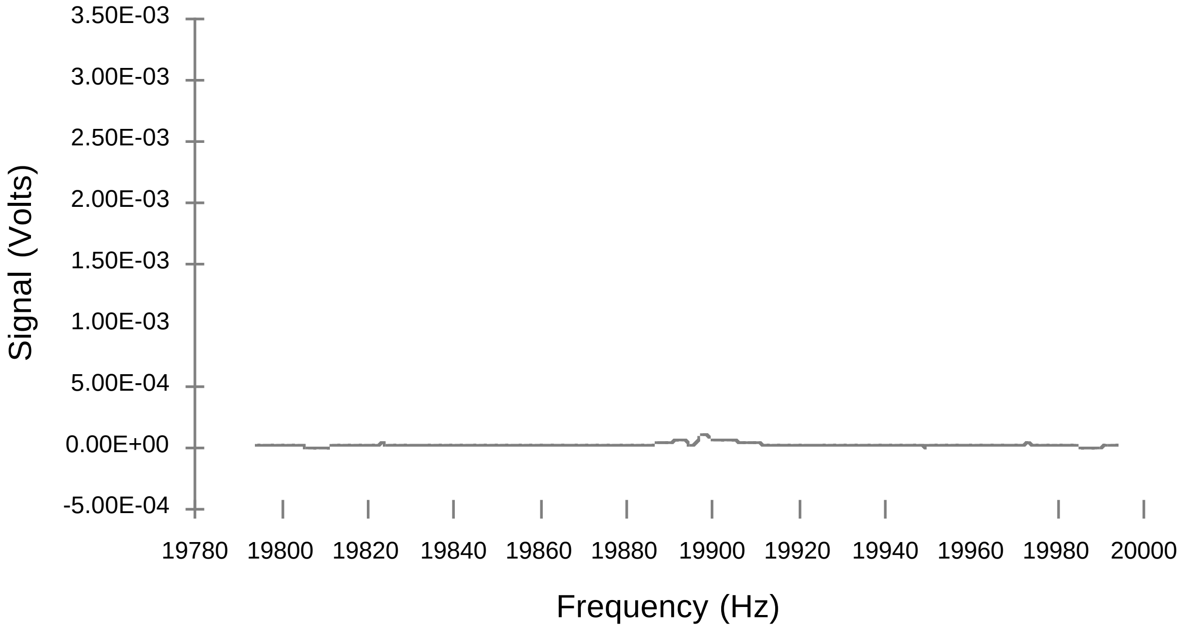

(a)

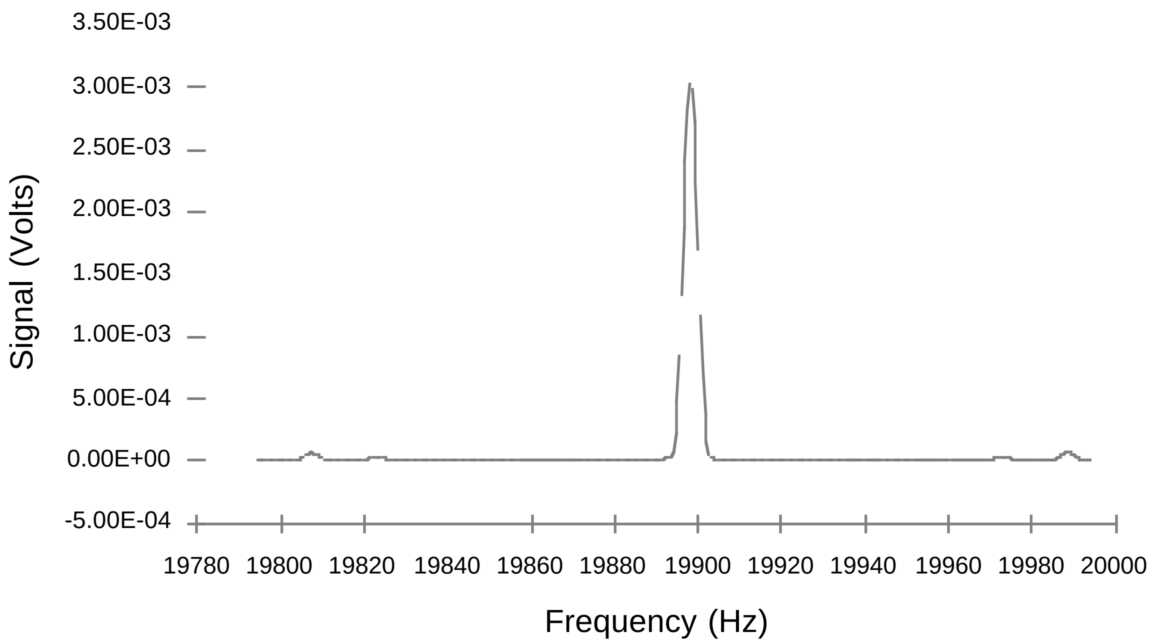

(b)

Figure 7. Zero background 20 kHz AM differential absorption measurements: a) Balanced modulation with no absorption, the sample etalon is off resonance. b) Sample etalon on resonance resulting in 3% differential absorption.

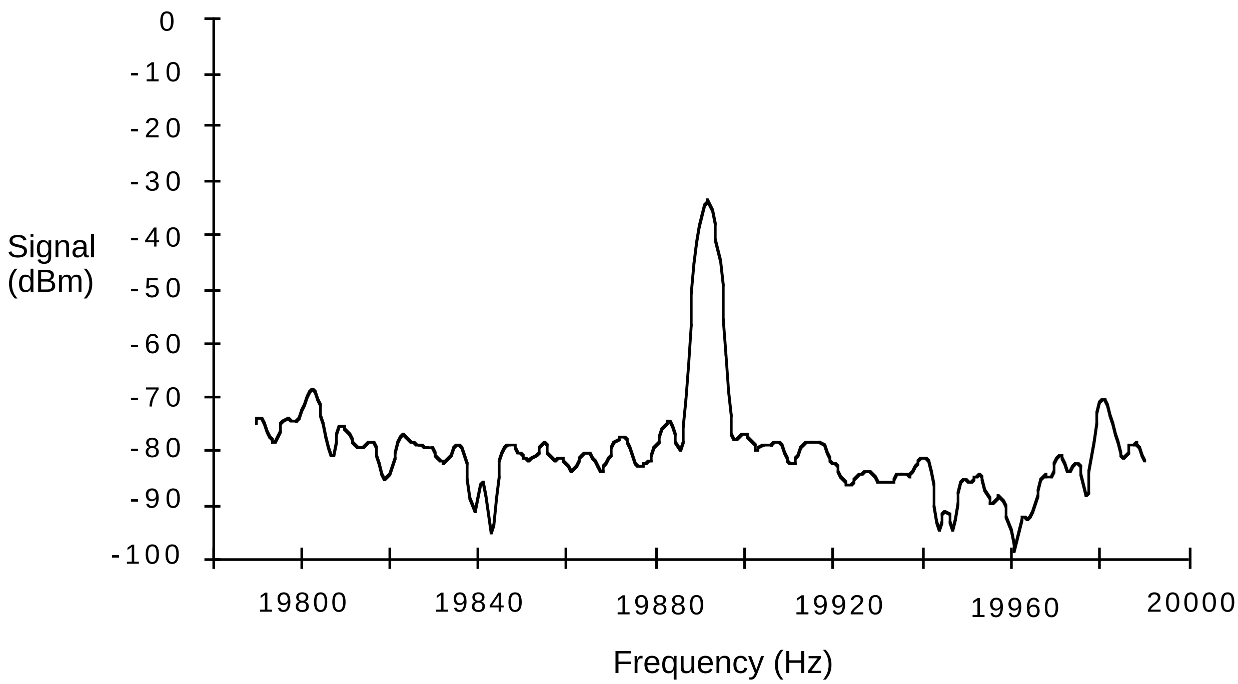

Figure 8. Log scale display of zero background AM signal for the 3% differential absorption shown in Figure 7b. Measurement details are given in the text.

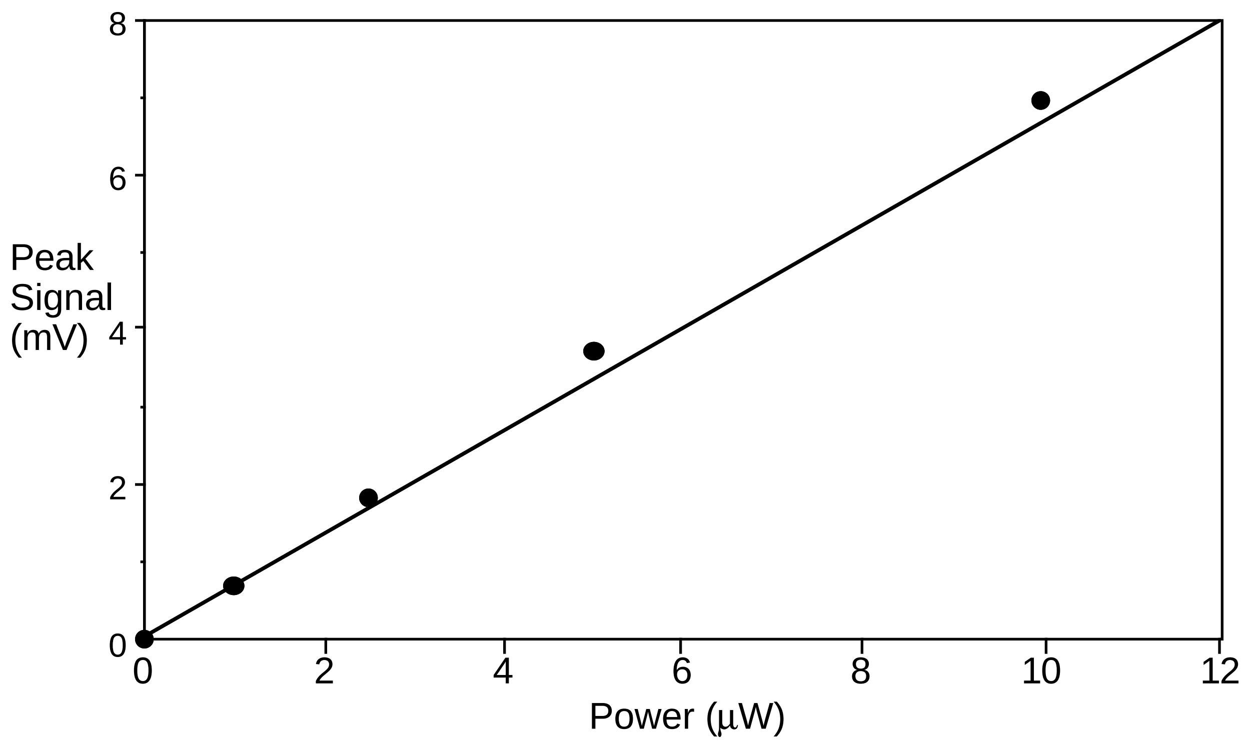

Figure 9. Measurement of the 20kHz AM signal linearity as a function of detected optical power for a 3% differential absorption. The solid line is a least squares fit to the data with a correlation coefficient of 0.998.

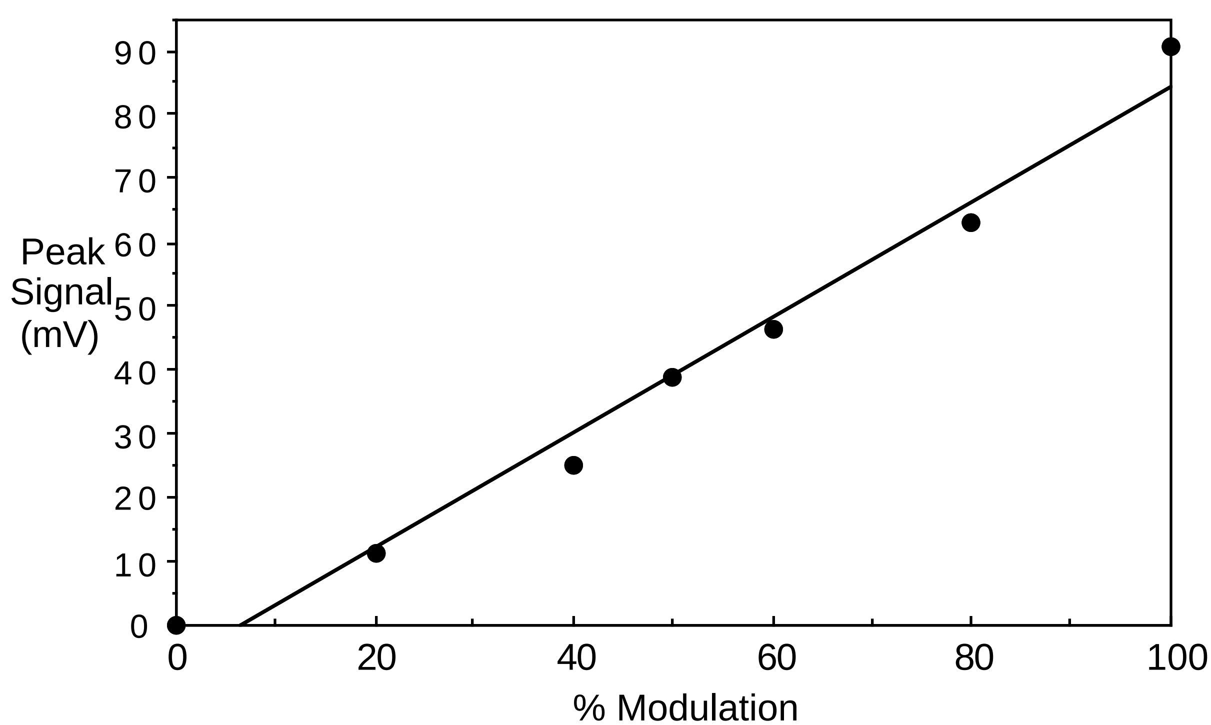

Figure 10. Measurement of the 20kHz AM absorption signal linearity as a function of the AM modulation index. The solid line is a least squares fit to the data with a correlation coefficient of 0.98.

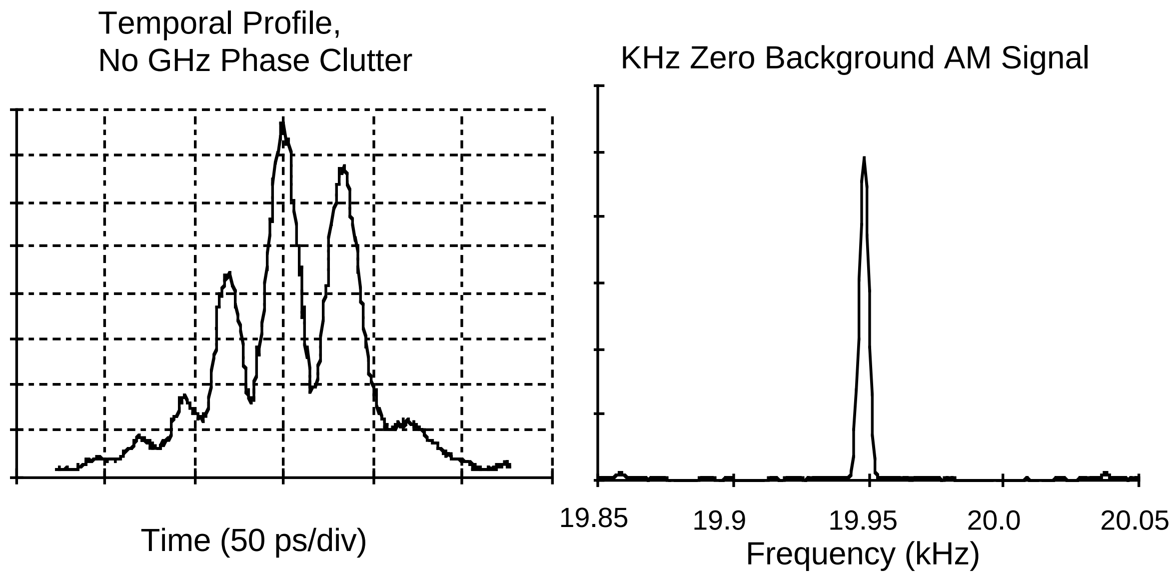

(a)

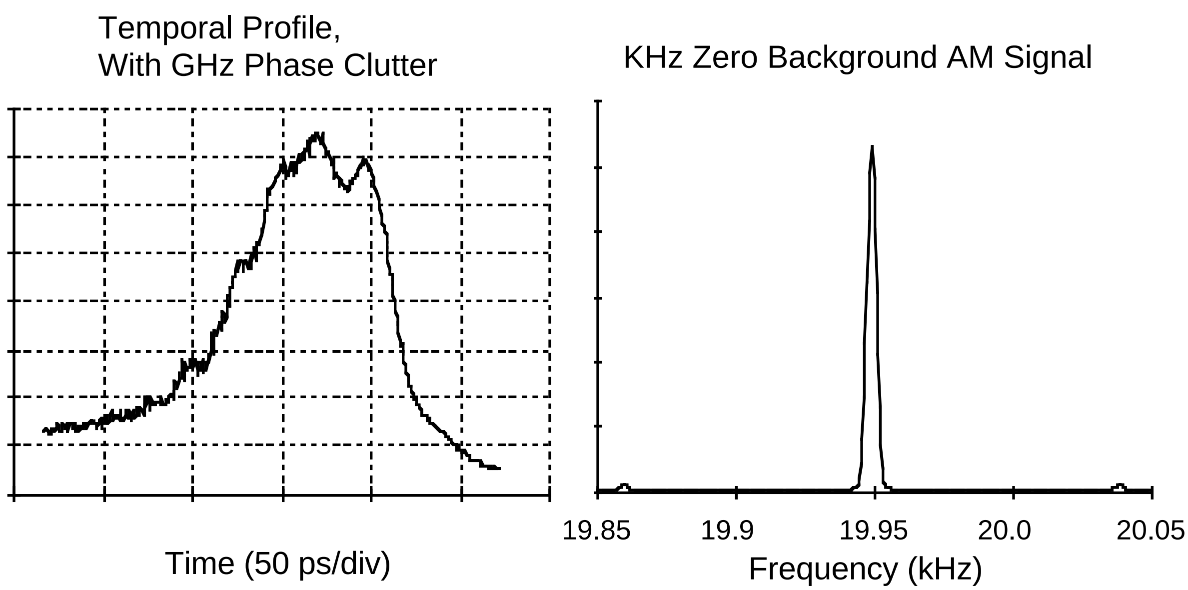

(b)

Figure 11. Results of fading experiments described in the text demonstrate the insensitivity of the AM signal to GHz phase clutter. (a) temporal and RF spectral profiles for 3% differential absorption signal. (b) temporal and RF spectral profiles in the presence of GHz phase clutter.

Technical Information Department • Lawrence Livermore National Laboratory
University of California • Livermore, California 94550